Proceedings of the 28th IEEE
EMBS Annual International Conference
New York City, USA, Aug 30-Sept 3, 2006

Near-infrared spectroscopic measurements of blood analytes using multi-layer perceptron neural networks

Dimitrios Kalamatianos*, Panos Liatsis† and Peter E. Wellstead*
*Hamilton Institute, National University of Ireland, Maynooth, Ireland
†School of Engineering and Mathematical Sciences, City University,
Northampton Square, London EC1V 0HB, UK

***Abstract*— Near-infrared (NIR) spectroscopy is being applied to the solution of problems in many areas of biomedical and pharmaceutical research. In this paper we investigate the use of NIR spectroscopy as an analytical tool to quantify concentrations of urea, creatinine, glucose and oxyhemoglobin (HbO_2). Measurements have been made *in vitro* with a portable spectrometer developed in our labs that consists of a two beam interferometer operating in the range of 800–2300 nm. For the data analysis a pattern recognition philosophy was used with a preprocessing stage and a multi-layer perceptron (MLP) neural network for the measurement stage. Results show that the interferogram signatures of the above compounds are sufficiently strong in that spectral range. Measurements of three different concentrations were possible with mean squared error (MSE) of the order of 10^{-6}.**

***Index Terms*— near-infrared spectroscopy, interferometer, neural networks, urea, creatinine, glucose, oxyhemoglobin**

I. INTRODUCTION

For clinical laboratory measurements, quantitative methods must be suitably accurate and precise over the expected range of values required. In addition, it is often desirable that the method be inexpensive, reliable, rapid and easily automated. Near-infrared spectroscopy has the potential to satisfy these criteria [1]. It needs no reagents, little or no sample preparation, it is rapid and nondestructive, and is suitable for complex matrices [2], [3]. Near-infrared spectroscopy has been applied to measuring urine composition [4], serum composition [5], fecal composition [6], glucose in whole blood [7] and complex matrices [8]. This paper explores the feasibility of the use of near-infrared analysis for measuring four compounds of interest for whole-blood screening testing. These compounds are: urea, creatinine, glucose and oxyhemoglobin. Their concentration levels in blood can indicate disease or organ dysfunction and their monitoring is of high importance in medicine and biology. High levels of urea, for example, indicate a problem with the removal, or more rarely with the over-production, of urea in the body. It is measured along with creatinine to indicate direct problems with the kidneys (e.g., chronic renal failure) or secondary problems such as hypothyroidism.

The conventional way of extracting information from spectroscopic data is by examining the spectra obtained and comparing spectral features with known absorption features of organic materials. In this paper we consider an alternative approach, in which a pattern learning philosophy is adopted for the analysis of interferogram domain data. Specifically, it is assumed that the interferogram (or spectrum) obtained with a particular material will have a specific signature. By learning the distinctive characteristics of such signature, we show how machine learning ideas and in particular feed-forward neural networks can be used to extract information and classify spectroscopic measurements.

II. INSTRUMENTATION

Spectra were collected with a novel Fourier transform (FT) Michelson interferometer developed in our lab [9] and operating in the NIR range. A schematic diagram of the instrument in transmission mode is shown in Fig. 1. White light passes through the sample and into the Michelson interferometer for analysis. Optical interference signals are generated from the light reflected from mirrors in the two arms of the interferometer. These signals are detected and pass via the detector amplifiers to the analogue to digital (A/D) boards of the supervisory computer. They are used to generate the interferogram and the next set of piezo-electric transducer (PZT) control signals. These are sent after digital to analogue (D/A) conversion to piezo drive circuits and after that to the PZT unit moving the mirror. Parallel to this, monochromatic laser signals are used for feedback control of the active mirror.

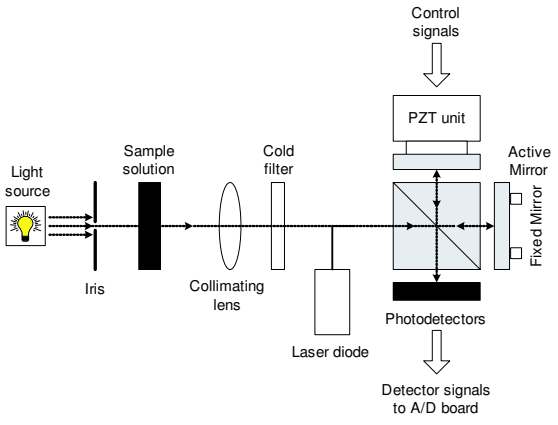

Fig. 1. Schematic diagram of the FT-NIR spectrometer in transmission mode.

The source used in this instrument was a quartz tungsten-halogen monofilament lamp, which has a useful operating

range of 220 nm to 2700 nm, i.e., from the ultraviolet through the visible band and into the infrared [10]. A 'cold filter' was inserted to low-pass filter the source, i.e., to remove the visible portion of the source spectrum and pass only wavelengths at the near-infrared region and above. At a distance of approximately 100 mm from the cold filter, a 20 mm fused silica corner cube beam-splitter assembly was located, by which the collimated source was amplitude-divided into the two arms of the interferometer. The moving mirror was securely fixed onto a piezo actuator subsystem (Piezosystem Jena, model 1058) and the fixed mirror was mounted on a rigid kinematic mount with three adjusting screws.

Perpendicular to the optical path, was a laser diode which had a wavelength of 670 nm and whose primary function was to provide the monochromatic fringes needed by the active alignment and alignment tracking algorithms. In addition, the laser also provided an accurate method of calibrating mirror displacement, which in turn was required to determine calibration of subsequent spectra wavelength measurements. In order to measure the amplitude of the laser fringes, four phototransistors, used as laser photo-detectors, were mounted in the detector head and positioned equidistantly around the main NIR detector. The devices selected were Sharp PT510, which have a typical response of 600–900 nm. The main photo-detector selected was a Hamamatsu P203 8-03 lead selenium (PbSe) device having a sensitivity range of 1 to 5 μm, integral thermistor and thermoelectric cooling plate.

III. EXPERIMENTAL

The samples and their concentrations are shown in Table I. The idea was to test for each compound a concentration close to its physiological level in blood and two more concentrations higher by 10 and 10^2 times as these were the first calibration tests of this kind. All solutions were made in the laboratory in physiologically buffered saline (PBS) and placed into a cuvette of 0.2 mm thickness. This cuvette was then put onto a sample holder between the light source and the interferometer as shown in Fig. 1. For generalization purposes, three samples of each concentration were measured, emptying the cuvette in between and 100 interferograms of 1024 data points from each sample were collected. Thus, the total number of interferograms collected from each compound, was $3\times3\times100$=900 and the data set $\mathbf{I}$ was defined as $\mathbf{I} \in \Re^{1024\times900}$.

TABLE I

CONCENTRATIONS OF SAMPLES MEASURED WITH THE PROTOTYPE INSTRUMENT.

Sample No	Concentrations (g/l)			
	Urea	Creatinine	Glucose	Oxyhemoglobin
1	0.25	0.015	0.01	1.5
2	0.25	0.015	0.01	1.5
3	0.25	0.015	0.01	1.5
4	2.5	0.15	0.1	15
5	2.5	0.15	0.1	15
6	2.5	0.15	0.1	15
7	25	1.5	1	150
8	25	1.5	1	150
9	25	1.5	1	150

IV. DATA ANALYSIS

Although, the inter-sample variation is not as great in the interferogram domain as in the wavelength domain [11], modeling in the interferogram domain offered a distinct advantage in terms of computational overheads, because the FT was not required. At first, the 900 interferograms were phase compensated to facilitate the averaging process and were therefore symmetrical about the centreburst. Thus, it was possible to truncate the data sets such that each contained only the data to the right of the centreburst, i.e., $\mathbf{I} \in \Re^{512\times900}$. The interferograms from each compound were then equally divided into training and test sets, $\mathbf{X}$ and $\mathbf{Z}$, consisting of 450 vectors each. In order to generalize the calibration, it was made sure that interferograms from all samples of each concentration were included. First, data were directly applied to *multi-layer perceptron* neural netowrks of various sizes and then several preprocessing techniques were tested for the extraction of analyte concentrations. In the case of untreated data, the number of inputs, i.e., data points presented to the network, was incremented from 1 to 20, and for each increment an MLP was simulated with one hidden layer, whose size was systematically varied between 1 and 30 nodes. For hidden layer nodes, hyperbolic tangent transfer functions were used, whereas logistic functions were used for output layer nodes. For each of the networks thus created, ten trials were attempted and the MSE of prediction and the number of epochs required by each were recorded. The criterion for stopping training was an MSE$<10^{-5}$ or an increment of the test error for a specified number of iterations. This is because the error on the test set begins to rise when the network begins to overfit the data. In all instances, the gradient descent with momentum and adaptive learning rate backpropagation algorithm [12] was used to train the networks.

In wavelength domain absorption spectroscopy, dividing the sample reflectance spectra by the source spectrum eliminates the adverse effects of the instrument function. An equivalent solution in the interferogram domain has been proposed in the form of *Gram-Schmidt orthonormalization* (GSO) [13]. In GSO, instrument variations are removed by projecting the training set of interferograms including one from the source onto an orthonormal subspace, which forms a basis onto which subsequent interferograms are projected and absorbancies determined by vector proximities.

A similar procedure to the one reported above for the direct presentation of interferometric data to MLPs of various sizes was repeated for data that had been pre-treated by *principal component analysis* (PCA) [14]. The intention was to determine the optimum network topology in terms of the number of inputs, i.e., principal components (PCs), and number of hidden nodes required. Another attempt to extract the true interferometric information was made with *hierarchical feature selection* (HFS) [15]. This method had

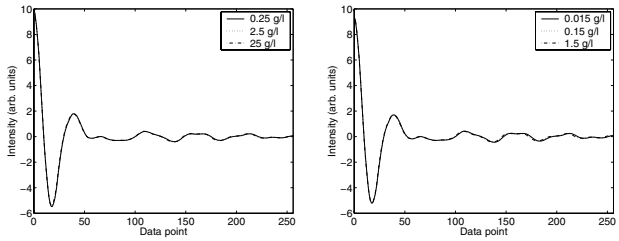

(a) Urea (b) Creatinine

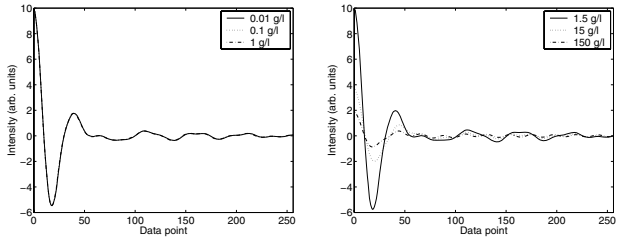

(c) Glucose (d) Oxyhemoglobin

Fig. 2. Plot of the mean interferograms of (a) urea, (b) creatinine, (c) glucose and (d) oxyhemoglobin obtained from the prototype instrument. The first 256 points to the right of the centreburst are shown.

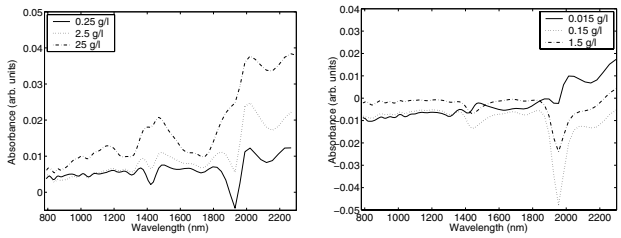

(a) Urea (b) Creatinine

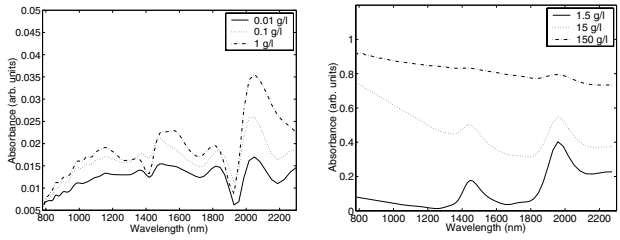

(c) Glucose (d) Oxyhemoglobin

Fig. 3. Plot of the mean absorption spectra of (a) urea, (b) creatinine, (c) glucose and (d) oxyhemoglobin obtained from the prototype instrument.

the advantage of reducing the dimensionality of the input space by replacing the most correlated pair of features by their average value. By repeating this process 256 times, half of the inputs remained finally. Here, again, a similar procedure as above was used to obtain the network with optimum topology using the new data matrices $\mathbf{X}, \mathbf{Z} \in \Re^{256\times 450}$.

V. RESULTS AND DISCUSSION

The first 256 points of the mean interferograms from each concentration are shown in Fig. 2 for urea, creatinine, glucose and oxyhemoglobin. It can be seen that the differences in the interferograms are more apparent in the case of oxyhemoglobin than the other three. This can be explained by having a closer look at Table I where it is shown that the concentrations of oxyhemoglobin are relative high in comparison with those of urea, creatinine and glucose. As a result, the differences of transmitted light through the creatinine and glucose samples are not so visible by eye.

In Fig. 3, the absorption spectra equivalent to the interferograms of Fig. 2 are plotted. Spectra from the reagent (PBS) were used as reference in order to produce the absorption spectra. The apparent negative absorbancies in the plots are most probably due to measurement errors or fluorescence effects caused by the re-emission of energy at intermediate energy levels [16]. It is noticeable from Figs. 2 and 3 that the inter-sample variation in the interferogram domain is not as great as that for the spectral domain, as expected.

In the case of directly applied data of urea, a network with 14 inputs and 27 hidden nodes gave an MSE of 1.2×10^{-2} which was the best for the trials attempted. GSO applied then to the data and the optimum topology was found to be 18-25-1, i.e., 18 inputs, 25 hidden nodes and 1 output. The MSE of prediction was not improved though, as it was 1.1×10^{-2}. Applying PCA and using 18 principal components and 26 hidden nodes, reduced the test error to 4.4×10^{-3}. The technique that gave the lowest prediction error was HFS. It also reduced the network's size to only 5 hidden nodes. Nine inputs were used and the test MSE was 3.75×10^{-5}. The above techniques repeated with the creatinine, glucose and oxyhemoglobin data and gave similar results which are summarized in terms of MSE and network topology in Table II. For all four compounds preprocessing with HFS improved the network performance, apart from HbO_2 where the measurement of concentrations was simple enough even with the unprocessed data. The MLP network outputs for 20 randomly chosen interferograms from the test set are shown with the corresponding target values in Fig. 4 for the case of HFS processed data from urea, creatinine, glucose and oxyhemoglobin solutions.

VI. CONCLUSIONS

This work demonstrated the utility of a novel Michelson interferometer operating in the near-infrared range of the spectrum for measurement of four important compounds of the human blood. NIR spectroscopy when combined with advanced signal processing techniques can produce precise and informative diagnostic information. To demonstrate this, dimensionality reduction techniques and multi-layer perceptron neural networks of various sizes were used to quantify different concentrations of urea, creatinine, glucose and oxyhemoglobin, measured with a prototype instrument *in vitro*. The mean squared prediction error of the best working algorithm was 8.43×10^{-6}. Further tests of the algorithms and instrument's development will include multi-variable analysis and *in vivo* measurements of blood and tissue. Our target is the use of small and robust NIR instrumentation with embedded disease diagnostic software for predictive and

TABLE II

SUMMARY OF EXPERIMENTAL RESULTS FROM THE OPTIMUM MODELS FOR MICHELSON BIOMEDICAL DATA.

		Preprocessing			
		None	GSO	PCA	HFS
Urea	Topology	14-27-1	18-25-1	18-26-1	9-5-1
	MSE	1.2×10^{-2}	1.1×10^{-2}	4.4×10^{-3}	3.75×10^{-5}
Creatinine	Topology	20-30-1	20-22-1	19-23-1	11-2-1
	MSE	1.76×10^{-2}	1.43×10^{-2}	6.5×10^{-3}	9.06×10^{-6}
Glucose	Topology	16-29-1	20-25-1	20-2-1	17-2-1
	MSE	1.86×10^{-2}	1.31×10^{-2}	1.3×10^{-3}	1.06×10^{-5}
HbO_2	Topology	5-23-1	6-27-1	3-27-1	2-28-1
	MSE	8.85×10^{-6}	5.68×10^{-6}	4.78×10^{-6}	8.43×10^{-6}

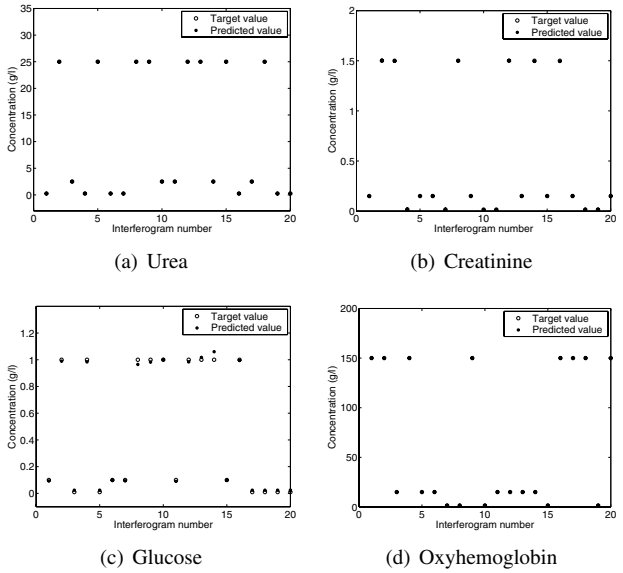

(a) Urea (b) Creatinine

(c) Glucose (d) Oxyhemoglobin

Fig. 4. Plot of the response of MLP to (a) urea, (b) creatinine, (c) glucose and (d) oxyhemoglobin interferograms from the prototype instrument preprocessed with HFS.

personalized medicine.

ACKNOWLEDGMENTS

The authors gratefully acknowledge the financial support of the Engineering and Physical Sciences Research Council and the Manchester Technology Fund. The contributions and assistance provided by Ralph J. Houston and Simon M. Christie are also greatly appreciated.

REFERENCES

[1] J. Pezzaniti, T.-W. Jeng, L. McDowell, and G. Oosta, "Preliminary investigation of near-infrared spectroscopic measurements of urea, creatinine, glucose, protein, and ketone in urine," *Clinical Biochemistry*, vol. 34, pp. 239–246, 2001.

[2] M. Arnold, "New developments and clinical impact of noninvasive monitoring," in *Handbook of Clinical Laboratory Automation, Robotics, and Optimization*, G. Kost, Ed. New York, NY: John Wiley & Sons, 1996, ch. 26, pp. 631–647.

[3] H. Heise, A. Bittner, and R. Marbach, "Clinical chemistry and near infrared spectroscopy: technology for non-invasive glucose monitoring," *Journal of Near Infrared Spectroscopy*, vol. 6, pp. 349–359, 1998.

[4] R. Shaw, S. Kotowich, H. Mantsch, and M. Leroux, "Quantitation of protein, creatinine, and urea in urine," *Clinical Biochemistry*, vol. 29, pp. 11–19, 1996.

[5] J. Hall and A. Pollard, "Near-infrared spectroscopic determination of serum total proteins, albumin, globulins, and urea," *Clinical Biochemistry*, vol. 26, pp. 483–490, 1993.

[6] G. Koumantakis and F. Radcliff, "Estimating fat in feces by near-infrared reflectance spectroscopy," *Clinical Chemistry*, vol. 34, pp. 502–506, 1987.

[7] S. Pan, H. Chung, and M. Arnold, "Near-infrared spectroscopic measurement of physiological glucose levels in variable matrices of protein and triglycerides," *Analytical Chemistry*, vol. 68, pp. 1124–1134, 1996.

[8] H. Heise, R. Marbach, G. Janatsch, and J. Kruse-Jarres, "Multivariate determination of glucose in whole blood by attenuated total reflection infrared scpectroscopy," *Analytical Chemistry*, vol. 61, pp. 2009–2015, 1989.

[9] D. Kalamatianos, J. Edmunds, P. Wellstead, R. Houston, P. Liatsis, S. Christie, R. Dewhurst, and M. Thorniley, "Dynamic alignment system for an FT-NIR Michelson interferometer," in *Proceedings of the IEEE International Conference on Virtual Environments, Human-Computer Interfaces and Measurement Systems*, Boston, MA, July 12-14 2004, pp. 120–124.

[10] J. Workman, Jr, *Applied Spectroscopy: A Compact Reference for Practitioners*. San Diego, CA: Academic Press, 1998, ch. Optical Spectrometers.

[11] B. Osborne, T. Fearn, and P. Hindle, *Practical NIR Spectroscopy*, 2nd ed. Harlow, UK: Longman Scientific and Technical, 1993.

[12] L. Fausett, *Fundamentals of neural networks: architectures, algorithms, and applications*. Upper Saddle River, NJ: Prentice-Hall, 1994.

[13] J. de Haseth and T. Isenhour, "Reconstruction of gas chromatograms from interferometric gas chromatography/infrared spectrometry data," *Analytical Chemistry*, vol. 49, no. 13, pp. 1977–1981, 1977.

[14] I. Jollife, *Principal Component Analysis*. New York, NY: Springer-Verlag, 1986.

[15] F. Ferri, J. Albert, I. Gracia, F. Pla, P. Pudil, and J. Novovičová, "Hierarchical feature selection: A decision tree based approach," in *Proceedings of AISB Workshop on Intelligent Feature Selection*, Brighton, UK, 1996, pp. 7–8.

[16] R. Ditchburn, *Light*. New York, NY: Dover Publications, 1991.